DOI: 10.1002/anie.201005613

Helical Transformations

Protonation-Triggered Conversion between Single- and Triple-Stranded Helices with a Visible Fluorescence Change**

*Xu-Hui Jin, Jian Wang, Jian-Ke Sun, Hong-Xing Zhang, and Jie Zhang**

Helical structures are ubiquitous in nature, and are essential and indispensable for various biological functions. Inspired by the elaborate functions of biological helices in molecular recognition, replication, translation, and catalytic activity, chemists have made great efforts to develop artificial helical polymers, supramolecules, and oligomers.[1] In particular, helical systems that can undergo conformational changes triggered by external stimuli are of significant attraction not only for gaining deep insight into the biological process, but also for the development of switchable systems that can be utilized in the biological and materials sciences.[2] Despite the great success in obtaining various single-helical architectures, the molecular designs for multi-stranded helical structures that consist of more than two strands are limited.[3] Although some synthetic helices have been shown conformational changes through the influence of external forces, such as solvent, pH, and temperature or ion binding,[3,4] the exploration is still in its infancy, and it remains a challenge to control the unwinding/rewinding or contraction/extension of helices optimally in water, as occurs in biological systems.[5]

A change in pH value is a crucial trigger for regulation of various functions of biosystems, such as biosensors, supramolecules, and drugs. The DNA triplex may be a pH-responsive nanomaterial in which an oligopyrimidine as the third strand associates with the corresponding DNA duplex by Hoogsteen hydrogen bonding under acidic conditions but dissociates to form the original duplex under basic conditions.[6] Although several pH-induced structural conversions have been reported for artificial helical systems to date, most of these occur in organic solvents and mainly involve the folding/unfolding molecular motions of single-stranded helices.[7] Recently, Yashima and co-workers found that the double helices of the oligoresorcinols formed in neutral aqueous solution were dissociated into single strands upon raising the pH.[8] However, the structural transition between single- and triple-helical conformation by pH manipulation has been rarely reported. Herein, we report the self-assembly of the single and triple helices driven by hydrogen-bonding interactions based on a flexible viologen derivative bearing two terminal carboxylic groups, and demonstrate how protonation can play a decisive role in the water-mediated helical transition by manipulating hydrogen bonding modes between the carboxyl groups. Attractively, this pH-dependent conformational conversion was accompanied by a fluorescence signal change, which can be directly visualized by the naked eye under a UV lamp at ambient conditions. Therefore the present system also can be regarded as a proton-triggered fluorescent switch.

A flexible viologen derivative, 1,1′-bis(2-carboxybiphenyl)-4,4′-bipyridinium dibromide, $(H_2Bcbpb)Br_2$, was synthesized by the route shown in Scheme 1. Treatment of the

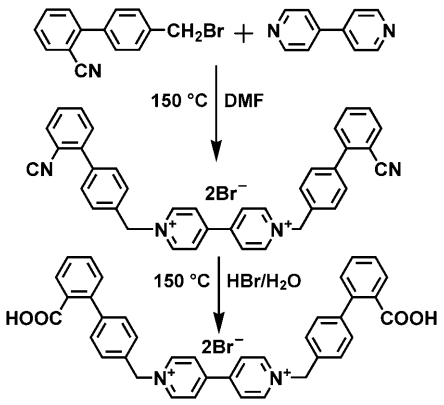

Scheme 1. Synthesis of the viologen derivative $(H_2Bcbpb)Br_2$.

dibromide salt with NaOH solution gave neutral zwitterionic viologen, which was further treated with aqueous solution of perchloric acid to afford crystals of $H_2Bcbpb{\cdot}2ClO_4{\cdot}H_2O$ (**S1**) and $HBcbpb{\cdot}ClO_4{\cdot}3H_2O$ (**T2**) at various pH values. The two samples are stable in air and dissolve sparingly in water at ambient temperature.

X-ray structure analysis reveals that different kinds of hydrogen bonds between carboxyl groups can be formed that link the bipyridinium molecules into single- or triple-stranded helices through exactly controlling the protonation of two carboxylate groups with perchloric acid. The bipyridinium molecules in **S1** are completely protonated. There is one H_2Bcbpb^{2+} dication, two perchlorate anions, and one lattice water molecule in the asymmetric unit. H_2Bcbpb^{2+} adopts a *trans* conformation with respect to the relative orientation of

[*] X.-H. Jin, J.-K. Sun, Prof. Dr. J. Zhang
State Key Laboratory of Structural Chemistry
Fujian Institute of Research on the Structure of Matter and
Graduate School of the Chinese Academy of Sciences
Fuzhou, Fujian 350002 (P.R. China)
Fax: (+86) 591-8371-0051
E-mail: zhangjie@fjirsm.ac.cn
J. Wang, Prof. Dr. H.-X. Zhang
State Key Laboratory of Theoretical and Computational Chemistry
Institute of Theoretical chemistry, Jilin University
ChangChun (P.R. China)

[**] This work was supported by the NNSF of China (Nos. 20671090/20973171), the NSF of Fujian Province (No. E0220003), and Key Project from CAS (KJCX2.YW.H01).

Supporting information for this article is available on the WWW under http://dx.doi.org/10.1002/anie.201005613.

the bipyridine group. The dihedral angles between the adjacent phenyl rings are 55.26 and 47.78°, whilst that between the pyridine rings is 33.90°. Interestingly, the adjacent carboxylic acid groups form a classic O–H···O hydrogen-bonded dimer with O···O distances of 2.679(8) and 2.654(8) Å in a $R_2^2(8)$ graph-set motif,[9] linking the H_2Bcbpb^{2+} cations into a single *meso*-helical structure which is characteristic of internal helix reversal (Figure 1a, b).

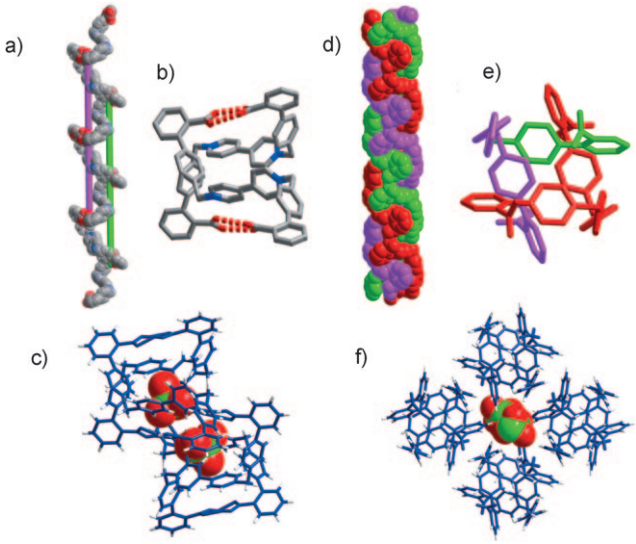

Figure 1. Structures of **S1** (a–c) and **T2** (d–f) from single-crystal X-ray determinations. a) A side view of the single-stranded *meso*-helix in **S1**; b) a top view of the single helix (C gray, O red, N blue); c) a top view showing the two neighboring single helices (C blue, H white) in which perchlorate ions (Cl green, O red) are located. d) A side view of the triple-stranded helix in **T2** (colors indicate strands); e) a top view of the triple helix; f) a top view showing the arrangement of triple helices among which perchlorate counterions are located.

Perchlorate anions are wrapped in the helical chain, stabilizing the helical structure and holding the adjacent helices together into a three-dimensional supramolecular framework through the C–H···O hydrogen bonds (Figure 1c). Meso-helices are widespread in nature, such as the tendrils of climbing plants, cycloamylose, and B/Z-DNA structures. However, in contrast to the well-studied common helices, *meso*-helical self-assembling systems still remain less explored.[10] To date, only a few organic examples of *meso*-helical structures have been characterized. Blay et al. reported the first organic example resulting from the solid-state aggregation of a dioxamic acid diester derivative,[10c] whilst Huc and co-workers presented the first example of rationally designed *meso*-helices that was obtained by using a strategy to control the relative orientation of two folded helical oligomers.[10d]

Compound **T2** crystallizes in the chiral space group and exhibits a triple-stranded helical structure. Its asymmetric unit is composed of one monoprotonated bipyridinium cation $HBcbpb^+$, one perchlorate anion, and three lattice water molecules. In contrast to **S1**, each $HBcbpb^+$ cation in **T2** adopts a *gauche* conformation in which the dihedral angles between the adjacent phenyl rings are 53.49 and 57.59°; the dihedral angle between the pyridine rings is 46.14°. A careful examination of the structure reveals the formation of strong COO^-···HOOC hydrogen bonds between adjacent carboxylate and carboxylic groups with a O···O distance of 2.507(4) Å. The $HBcbpb^+$ cations are linked into an infinite strand extending along the *a* axis direction through these hydrogen bonds. The helical pitch, given by the distance between equivalent atoms generated by one full rotation of the twofold screw axis, is 41.11 Å. Attractively, the three single-stranded infinite helices are of the same *M* handedness and are intertwined to form a chiral infinite triple-helical structure (Figure 1d, e). The repeat distance of the braid (13.70 Å) is one-third of a single helix pitch, which corresponds to the *a* axis length. Although some organic triple helices have been structurally characterized to date,[3a,11] the formation of a supramolecular triple helix through self-assembly of an achiral building block based on hydrogen bonding interactions is still rare. It is of interest to note that all of the helices are of the same chirality and are packed in a parallel manner, leading to a non-centrosymmetric and chiral supramolecular framework (Figure 1f). The hydrogen bonds between the lattice water molecules and carboxyl oxygen atoms, as well as the short C–H···O hydrogen-bonding interactions between perchlorate counterions and the aromatic rings (3.14–3.22 Å) serve as the driving force for this parallel packing.

Interestingly, different protonated forms of Bcbpb molecule render distinct luminescence characteristics to these two crystals. **T2** does not exhibit a discernable luminescence signal in solid or solution upon excitation with UV light, whereas crystals of **S1** appear very bright to the eye with a yellow-green color under a UV lamp at ambient conditions. This visual observation can be verified by a fluorescence spectroscopy measurement, which exhibits a broad peak in the range of 420–750 nm with a maximum at about 522 nm and a small peak centered at 380 nm upon excitation at 275 nm. Furthermore, **S1** also emits detectable fluorescence in diluted solution. From Figure 2, it can be seen that the photoluminescence spectrum of **S1** in CH_3CN exhibits a main emission peak around 551 nm accompanied by a weak emission at 358 nm. The H_2Bcbpb^{2+} cation possesses both carboxybiphenyl donor and bipyridinium acceptor units, which are approximately perpendicular to each other in its crystal structure. From the fluorescence emission of **S1** in different solvents, the intense low-energy emission band undergoes obvious red-shift with increasing solvent polarity (more than 100 nm on going from THF to CH_3CN). This solvent-dependent luminescence behavior is similar to the twisted intramolecular charge-transfer (TICT) emission feature as observed for some donor–acceptor molecules;[12] therefore, the TICT-like mechanism is thought to be involved in present photoluminescence system. For viologen derivatives, controversy exists concerning their fluorescence properties. It has been often reported that the methyl viologen dication is not fluorescent in fluid solutions.[13] However, a fluorescence emission around 350 nm has been repeatedly observed by several groups for the bipyridinium derivatives in some solvents, although quantum yields were still low.[13] The short

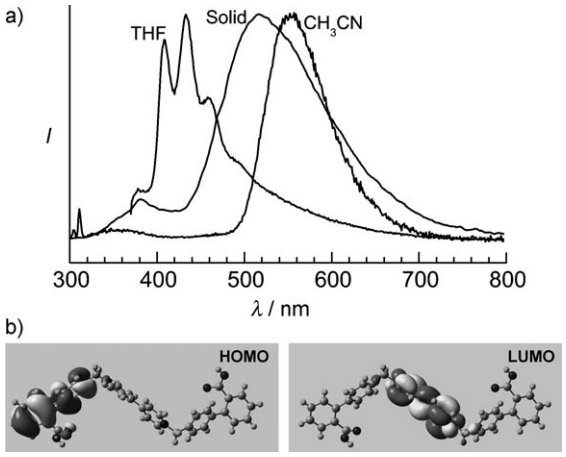

Figure 2. a) Normalized fluorescence emission spectra of **S1** in CH_3CN at 2.5×10^{-5} M, THF solutions at 1×10^{-5} M ($\lambda_{ex}=285$ nm), and in the solid state ($\lambda_{ex}=275$ nm). b) The calculated spatial distributions of the LUMO and the HOMO of **S1**.

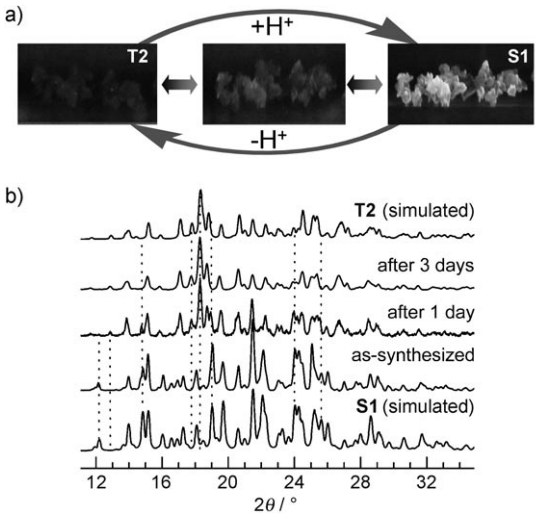

Figure 3. a) Photographs taken under 365 nm UV light illumination at room temperature to show the stepwise change in fluorescence emission upon water-mediated solid-state interconversion. b) The transformation of **S1** into **T2** in water as observed by powder X-ray diffraction.

wavelength band observed in our experiments corresponds well to this emission band.

For a better understanding of the photophysical processes of **S1**, molecular orbital calculations were performed using the Gaussian suite of programs (Gaussian 09) and the basis set TD-TPSSh/6-311G(d). The ground state geometry was adapted from the X-ray data. The calculation results showed that **S1** exhibited the complete separation of the HOMO and the LUMO (Figure 2b). The majority of the electron distribution of the HOMO was located on the 2-carboxybiphenyl moiety; that of the LUMO was concentrated on the bipyridinium moiety. The complete localization of HOMO and LUMO means the HOMO–LUMO transition becomes a typical photoinduced intramolecular charge transfer transition,[14] which is consistent with our experimental findings.

Interestingly, the two kinds of crystals exhibit luminescence that variously fade away or grow when they are immersed in distilled water or perchloric acid solution, respectively. The photographs given in Figure 3a clearly manifest the transition between non-emission and emission for these crystals. Crystals of **S1** exhibit brilliant luminescence under 365 nm UV light at the beginning of the immersion in water. With increasing immersion time, the luminescence is found to fade away quickly, and then is barely discernible after 24 h. In contrast, the non-luminescent triple-helical compound displays a gradually enhanced fluorescence emission when it is allowed to stand for as long as 12 h in the perchloric acid solution with pH 1. These results indicate that two compounds may undergo a conformational interconversion between one helix to another in response to changes in pH.

The direct evidence for the transformation between the two kinds of helical structures comes from powder X-ray diffraction (PXRD) analyses (Figure 3b). The PXRD pattern of the original sample **S1** shows excellent agreement with the simulated pattern obtained from the single-crystal structure data. After the original sample was immersed in distilled water for one day, several noticeable variations could be discerned. Some reflections at 2θ values of 12.20, 18.06, and 25.62° disappeared; whilst new reflections appeared at 2θ values of 12.86, 17.76, and 18.30°, which were in good agreement with the simulated reflection peaks of **T2**. Upon continuing immersion for two additional days, some reflections underwent small position shifts towards the evolvement to **T2**, and the reflections at 2θ values of 14.74, 19.02, and 23.92° also disappeared. All of the diffraction peaks of the sample were found to exhibit good agreement with those of **T2**, meaning that the single-helical structure of **S1** has been completely transformed into the triple-helical structure. For **T2**, after the original sample was immersed in the perchloric acid solution for two days, the reflections at the 2θ values of 17.24, 18.36, 20.78, and 23.12° disappeared. Additionally, beside the indicative peaks for **S1** occurring at 2θ values of 22.06 and 25.58°; a new reflection at $2\theta=26.30°$, which corresponds to none of the simulated peaks of the two compounds, can also be found. This observation seems to indicate that an intermediate state was formed during the transformation from **T2** to **S1**. Upon further treatment with the perchloric acid solution for 12 days, all of the diffraction peaks of the sample agreed with the simulated PXRD pattern of **T2** (Figure 2S in the Supporting Information). This result indicates that the helical transition of **T2** is induced by protonation. No solubility phenomenon was observed during the transformation owing to the low solubility of **S1** and **T2** in water; therefore, the whole process can be regarded as a water-mediated solid-state conversion.

The transformation process between single- and triple-helical structures can also be further identified based on IR spectral analysis. As shown in Figure 4, the as-synthesized sample **S1** exhibits a strong peak at 1692 cm^{-1} that can be assigned to the antisymmetric C=O stretching vibration of the hydrogen-bonded carboxylic acid dimer,[15a] corresponding

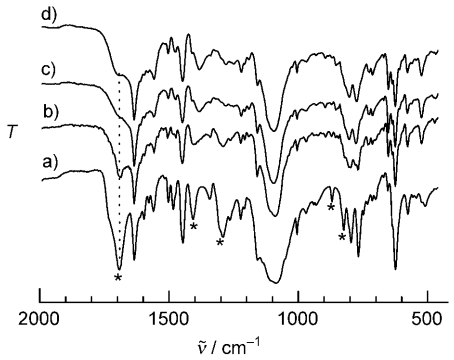

Figure 4. The transformation of **S1** into **T2** in water as observed by IR spectroscopy. a) as-synthesized **S1**; b) immersion for 1 day; c) immersion for 3 days; d) as-synthesized **T2**. The peaks marked with asterisks undergo significant changes during the transformation process.

well to the structural analysis results. Upon immersing the sample into water, the intensity of this vibration band gradually decreased, and eventually evolved into a shoulder as observed in the spectrum of **T2**. Other vibration bands underwent small position shifts or fading, reaching an agreement with those in **T2** after immersion for three days. In contrast, a decrease in the intensity of the band around 1690 cm^{-1} and the presence of carboxylate symmetric 1383 cm^{-1} (ν_s COO$^-$) band[15] in **T2** indicates different protonated forms between two kinds of crystals. After the treatment with perchloric acid for two days, an intense new band at 1720 cm^{-1} (corresponding to the carboxylic acid without dimerization) can be clearly observed, suggesting the formation of an intermediate state during the transformation of **T2**. This result is in accordance with the PXRD observation. After 12 days, the intensity of the band at 1720 cm^{-1} decreased considerably, whilst the band at 1692 cm^{-1} became dominant, accompanied with the general profile resembling that of **S1** (Figure 3S in the Supporting Information). Incomplete fading of the vibration band at 1720 cm^{-1} together with long transformation time suggest that the transformation from triple helix **T2** to single helix **S1** is more difficult to realize than that from **S1** to **T2**. In fact, although a complete transformation is easy to achieve in hydrothermal condition, the transformation from **T2** to **S1** at room temperature is not always successful in several repeated experiments, which is quite different from that from **S1** to **T2**. The appearance of an intermediate state during protonation should be mainly responsible for this predicament. The carboxyl group as a typical functional group is essential for the biological activity of the protein; it has been suggested that the carboxylic acid hydrogen bonds play a crucial role in the mechanism of HIV protease.[16] The different transformation pathways (Figure 5) observed in the winding/unwinding of the present system clearly demonstrate the complexity of protonation phenomena and the decisive effect of hydrogen bond orientation on supramolecular conformations.

In conclusion, we have presented the unique self-assembly of the single- and triple-stranded helices driven by hydrogen-bonding interactions based on a flexible viologen carboxylic derivative. The pH-triggered transformation of two helical conformations can be achieved by a water-mediated solid-state phase conversion by different pathways, which demonstrates an important role of protonation in the helical transition by manipulating hydrogen bonding modes between the carboxyl groups. Attractively, this pH-dependent conformational conversion is accompanied by a visual fluorescence change. These results provide not only a valuable insight into the mechanism for the construction and conversion of helical structures, but also a promising approach to the development of supramolecular systems undergoing structural changes induced by external stimuli, and pH-sensitive materials.

Received: September 8, 2010
Published online: December 22, 2010

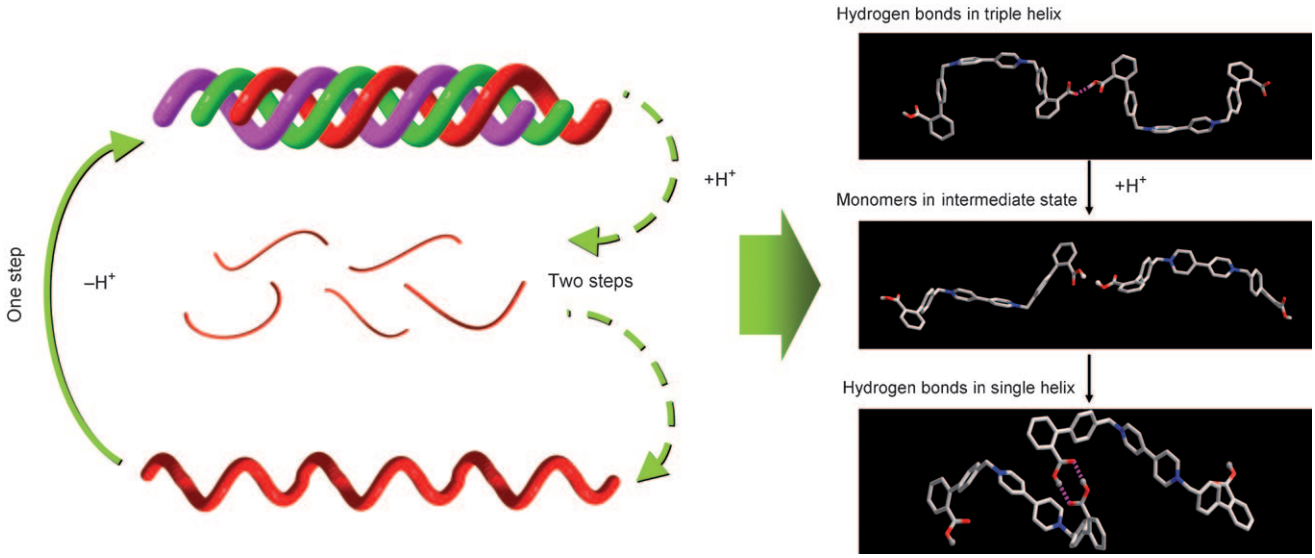

Figure 5. Illustration of the helix transformation between **S1** and **T2** regulated by protonation/deprotonation through water-mediated solid-state conversion at room temperature.

Keywords: fluorescence · helical structures · hydrogen bonds · structural transformations · viologen

[1] a) E. Yashima, K. Maeda, H. Iida, Y. Furusho, K. Nagai, *Chem. Rev.* **2009**, *109*, 6102 – 6211; b) E. Yashima, K. Maeda, Y. Furusho, *Acc. Chem. Res.* **2008**, *41*, 1166 – 1180; c) D. Haldar, C. Schmuck, *Chem. Soc. Rev.* **2009**, *38*, 363 – 371.

[2] a) S. Chakraborty, S. Sharma, P. K. Maiti, Y. Krishnan, *Nucleic Acids Res.* **2009**, *37*, 2810 – 2817; b) G. Z. Yuan, C. F. Zhu, Y. Liu, W. M. Xuan, Y. Cui, *J. Am. Chem. Soc.* **2009**, *131*, 10452 – 10460; c) T. Yamada, Y. Nagata, M. Suginome, *Chem. Commun.* **2010**, *46*, 4914 – 4916; d) H. Sugiura, R. Amemiya, M. Yamaguchi, *Chem. Asian J.* **2008**, *3*, 244 – 260; e) E. Kolomiets, V. Berl, J.-M. Lehn, *Chem. Eur. J.* **2007**, *13*, 5466 – 5479; f) H.-J. Kim, E. Lee, H.-s. Park, M. Lee, *J. Am. Chem. Soc.* **2007**, *129*, 10994 – 10995.

[3] a) Y. Ferrand, A. M. Kendhale, J. Garric, B. Kauffmann, I. Huc, *Angew. Chem.* **2010**, *122*, 1822 – 1825; *Angew. Chem. Int. Ed.* **2010**, *49*, 1778 – 1781; b) H. Ito, Y. Furusho, T. Hasegawa, E. Yashima, *J. Am. Chem. Soc.* **2008**, *130*, 14008 – 14015; c) H. Yamada, K. Maeda, E. Yashima, *Chem. Eur. J.* **2009**, *15*, 6794 – 6798; d) Y. Furusho, E. Yashima, *J. Polym. Sci. Part A* **2009**, *47*, 5195 – 5207; e) M. Ikeda, S. Haraguchi, M. Numata, S. Shinkai, *Chem. Asian J.* **2007**, *2*, 1290 – 1298.

[4] K. Miwa, Y. Furusho, E. Yashima, *Nat. Chem.* **2010**, *2*, 444 – 449.

[5] a) H. Goto, Y. Furusho, E. Yashima, *J. Am. Chem. Soc.* **2007**, *129*, 109 – 112; b) J. G. Kennemur, J. B. Clark IV, G. L. Tian, B. M. Novak, *Macromolecules* **2010**, *43*, 1867 – 1873.

[6] K.-i. Haruna, H. Iida, K. Tanabe, S.-i. Nishimoto, *Org. Biomol. Chem.* **2008**, *6*, 1613 – 1617.

[7] a) H. Goto, Y. Furusho, E, Yashima, *Chem. Commun.* **2009**, 1650 – 1652; b) C. Dolain, V. Maurizot, I. Huc, *Angew. Chem.* **2003**, *115*, 2844 – 2846; *Angew. Chem. Int. Ed.* **2003**, *42*, 2738 – 2740; c) E. Kolomiets, V. Berl, I. Odriozola, A.-M. Stadler, N. Kyritsakas, J.-M. Lehn, *Chem. Commun.* **2003**, 2868 – 2869.

[8] H. Goto, Y. Furusho, K. Miwa, E. Yashima, *J. Am. Chem. Soc.* **2009**, *131*, 4710 – 4719.

[9] M. C. Etter, *Acc. Chem. Res.* **1990**, *23*, 120 – 126.

[10] a) J. J. Jiang, S. R. Zheng, Y. Liu, M. Pan, W. Wang, C. Y. Su, *Inorg. Chem.* **2008**, *47*, 10692 – 10699; b) J. C. Jin, Y. Y. Wang, P. Liu, R. T. Liu, C. Ren, Q. Z. Shi, *Cryst. Growth Des.* **2010**, *10*, 2029 – 2032; c) G. Blay, I. Fernández, J. Pedro, R. Ruiz-García, M. C. Muñoz, J. Cano, R. Carrasco, *Eur. J. Org. Chem.* **2003**, 1627 – 1630; d) V. Maurizot, C. Dolain, Y. Leydet, J.-M. Léger, P. Guionneau, I. Huc, *J. Am. Chem. Soc.* **2004**, *126*, 10049 – 10052.

[11] a) H. Katagiri, Y. Tanaka, Y. Furusho, E. Yashima, *Angew. Chem.* **2007**, *119*, 2487 – 2491; *Angew. Chem. Int. Ed.* **2007**, *46*, 2435 – 2439; b) A. K. Das, D. Haldar, R. P. Hegde, N. Shamala, A. Banerjee, *Chem. Commun.* **2005**, 1836 – 1838; c) M. P. Lightfoot, F. S. Mair, R. G. Pritchard, J. E. Warren, *Chem. Commun.* **1999**, 1945 – 1946; d) X. Ouyang, F. W. Fowler, J. W. Lauher, *J. Am. Chem. Soc.* **2003**, *125*, 12400 – 12401; e) M. Albrecht, *Top. Curr. Chem.* **2004**, *248*, 105 – 139, and references therein.

[12] a) E. Lager, J. Z. Liu, A. Aguilar-Aguilar, B. Z. Tang, E. Peña-Cabrera, *J. Org. Chem.* **2009**, *74*, 2053 – 2058; b) Y. Sato, M. Morimoto, H. Segawa, T. Shimidzu, *J. Phys. Chem.* **1995**, *99*, 35 – 39; c) R. G. Hu, E. Lager, A. Aguilar-Aguilar, J. Z. Liu, J. W. Y. Lam, H. H. Y. Sung, I. D. Williams, Y. C. Zhong, K. S. Wong, E. Peña-Cabrera, B. Z. Tang, *J. Phys. Chem. C* **2009**, *113*, 15845 – 15853; d) L. N. Zhu, C. Zhong, Z. Y. Liu, C. L. Yang, J. G. Qin, *Chem. Commun.* **2010**, *46*, 6666 – 6668.

[13] a) R. Ballardini, A. Credi, M. T. Gandolfi, C. Giansante, G. Marconi, S. Silvi, M. Venturi, *Inorg. Chim. Acta* **2007**, *360*, 1072 – 1082; b) J. Peon, X. Tan, J. D. Hoerner, C. Xia, Y. F. Luk, B. Kohler, *J. Phys. Chem. A* **2001**, *105*, 5768 – 5777, and references therein.

[14] H. Y. Li, Z. G. Chi, B. J. Xu, X. Q. Zhang, Z. Y. Yang, X. F. Li, S. W. Liu, Y. Zhang, J. R. Xu, *J. Mater. Chem.* **2010**, *20*, 6103 – 6110.

[15] a) D. Lin-Vien, N. B. Colthup, W. G. Fately, J. G. Grasselli, *The Handbook of Infrared and Raman Characteristic Frequencies of Organic Molecules*, Academic Press, Sandiego, **1991**, p. 137 – 141; b) Md. K. Nazeeruddin, R. Humphry-Baker, P. Liska, M. Grätzel, *J. Phys. Chem. B* **2003**, *107*, 8981 – 8987.

[16] a) Y. Kiso, H. Matsumoto, S. Yamaguchi, T. Kimura, *Lett. Pept. Sci.* **1999**, *6*, 275 – 281; b) A. Brik, C.-H. Wong, *Org. Biomol. Chem.* **2003**, *1*, 5 – 14.

